

# The role of structural changes in the excitation of chemical waves in the system Rh(110)/NO+H<sub>2</sub>

Cite as: J. Chem. Phys. **106**, 4319 (1997); <https://doi.org/10.1063/1.473133>

Submitted: 10 June 1996 . Accepted: 27 November 1996 . Published Online: 04 June 1998

F. Mertens, S. Schwegmann, and R. Imbihl



View Online



Export Citation

## ARTICLES YOU MAY BE INTERESTED IN

[Modeling anisotropic chemical wave patterns in the NO+H<sub>2</sub> reaction on a Rh\(110\) surface](#)

The Journal of Chemical Physics **114**, 9083 (2001); <https://doi.org/10.1063/1.1362691>

[Existence diagram for chemical wave patterns in the NO+H<sub>2</sub> reaction on Rh\(110\)](#)

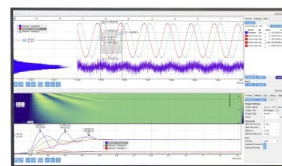
The Journal of Chemical Physics **107**, 4741 (1997); <https://doi.org/10.1063/1.474835>

[Chemical waves in the O<sub>2</sub> + H<sub>2</sub> reaction on a Rh\(111\) surface alloyed with nickel. I. Photoelectron emission microscopy](#)

The Journal of Chemical Physics **148**, 154704 (2018); <https://doi.org/10.1063/1.5020372>

Challenge us.

What are your needs for periodic signal detection?



Zurich  
Instruments



# The role of structural changes in the excitation of chemical waves in the system Rh(110)/NO+H<sub>2</sub>

F. Mertens<sup>a)</sup> and S. Schwegmann

*Fritz-Haber-Institut der Max-Planck-Gesellschaft, Faradayweg 4-6, D-14195 Berlin, Germany*

R. Imbihl<sup>b)</sup>

*Institut für Physikalische Chemie und Elektrochemie, Universität Hannover, Callinstr. 3-3a, D-30167 Hannover, Germany*

(Received 10 June 1996; accepted 27 November 1996)

Previous investigations have demonstrated that the formation of chemical waves in the NO+H<sub>2</sub> reaction on Rh(110) involves a cyclic transformation of the surface structure via various N,O-induced reconstructions, i.e., starting from the  $c(2\times6)$ -O a cycle is initiated comprising the formation of a  $(2\times3)/(3\times1)$ -N and a mixed  $c(2\times4)$ -2O,N structure. The stability and reactivity of these structures has been investigated in titration experiments as well as under stationary reaction conditions employing LEED, work function, rate measurements, and thermal desorption spectroscopy. It was shown that the  $c(2\times6)$ -O and  $c(2\times4)$ -2O,N structures exhibit a low reactivity whereas the  $(2\times1)/(2\times1)$ -N displays only a small to moderate decrease in catalytic activity ( $\approx 20\% - 30\%$ ) compared to the clean surface. On the basis of these results, an excitation mechanism for pulses in the NO+H<sub>2</sub> reaction on Rh(110) was constructed consisting of the sequence  $c(2\times6)$ -O,  $(2\times1)/(3\times1)$ -N  $c(2\times4)$ -2O,N,  $c(2\times6)$ -O. © 1997 American Institute of Physics. [S0021-9606(97)01409-8]

## I. INTRODUCTION

The interaction of NO with a Rh(110) surface is of interest not only because of the key role rhodium has in the automotive catalytic converter for reducing NO<sub>x</sub> emissions, but also with respect to a number of scientific aspects. The dissociation products atomic oxygen and nitrogen generate a large number of different adsorbate-induced reconstructions which have been in the focus of investigations with scanning tunneling microscopy (STM) and LEED.<sup>1-9</sup> In the NO+H<sub>2</sub> reaction on Rh(110) recently chemical wave patterns of rectangular shape were observed whose origin was traced back to the different anisotropies of the O- and N-induced reconstructions on this surface.<sup>10-15</sup>

The chemical wave patterns were found at  $p \approx 10^{-5}$  mbar in a  $T$ -range from  $\approx 480$  to 650 K.<sup>14</sup> In a parameter range which is smaller with respect to  $p_{\text{H}_2}$  rate oscillations could be observed under conditions under which gas-phase coupling synchronized the reacting Rh(110) surface.<sup>15</sup> A second oscillatory  $T$ -range exists at higher temperature at  $\approx 900$  K; in this range rate oscillations were found in the NO+CO and in the NO+H<sub>2</sub> reaction on Rh(110).<sup>16-18</sup> On other Rh surface orientations oscillatory behavior was detected too. In field electron microscopy (FEM) studies in the group of Nieuwenhuys it was shown that in the NO+H<sub>2</sub> and NO+NH<sub>3</sub> reaction regularly shaped reaction fronts periodically spread out over the surface of a Rh field emitter tip.<sup>19,20</sup> Subsequent single crystal experiments demonstrated that rate oscillations in the NO+H<sub>2</sub> reaction occurred on Rh(533) but not on Rh(100).<sup>21,22</sup> A photoelectron emission microscopy (PEEM)

study of the NO+H<sub>2</sub> reaction on Rh(111) showed traveling pulses similar to Rh(110) but with isotropic wave propagation.<sup>23</sup>

For none of the abovementioned reaction systems an experimentally verified oscillation mechanism exists. The rectangularly shaped chemical wave patterns on Rh(110) were successfully reproduced with a mathematical model, but these simulations were carried out with a general model for excitable media and not with a specific model for Rh(110)/NO+H<sub>2</sub>.<sup>11,13</sup> Most of the difficulties in establishing a realistic model can be traced back to the problem of quantifying the role of subsurface oxygen and nitrogen and to the limited knowledge about the reactivity of the various substrate reconstructions.

A significant number of studies have been conducted with the Rh(110) surface dealing with the geometry and the stability of the various N- and O-induced reconstructions.<sup>1-9,24-28</sup> In a number of thermal desorption experiments it was demonstrated that the stability of a nitrogen adlayer on Rh(110) is strongly influenced by coadsorbed oxygen such that large amounts of oxygen have a destabilizing effect while small amounts of oxygen stabilize the N-layer.<sup>24-28</sup> These effects provide a feedback mechanism with which one can construct an oscillatory cycle.

In previous investigations the existence range for spatiotemporal pattern formation in parameter space has been mapped out and *in situ* LEED experiments showed the involvement of various N- and O-induced reconstructions.<sup>14</sup> Pattern formation in the NO+H<sub>2</sub> reaction and also in the bistable O<sub>2</sub>+H<sub>2</sub> reaction on Rh(110) has been investigated in detail.<sup>10-15,29</sup> In this paper we study the stability of the various adsorbate-induced reconstructions involved in the propagation of chemical waves in titration experiments and under

<sup>a)</sup>Present address: Center for Nonlinear Dynamics, University of Texas, Austin, Texas 78712.

<sup>b)</sup>Author to whom correspondence should be addressed.

stationary reaction conditions. Based on these experiments we can construct a plausible sequence for the structural transformations in a chemical wave for the system Rh(110)/NO+H<sub>2</sub>. The oscillation mechanism, however, is insofar incomplete as we leave out a possible role of subsurface oxygen/nitrogen which remains to be shown in further investigations.

## II. EXPERIMENT

The experiments were performed in two standard UHV chambers pumped with combinations of turbomolecular pump/titanium sublimation pump. All experiments under stationary conditions were conducted in a chamber equipped with LEED, a scanning Auger electron spectrometer, a photoelectron emission microscope (PEEM), a Kelvin probe, a differentially pumped quadrupole mass spectrometer (QMS) for rate measurements, and a feedback-stabilized gas inlet system. The titration and thermal desorption spectroscopy (TDS) experiments were carried out in a second chamber equipped with LEED, a piezo-driven Kelvin probe for work function measurements and a QMS with which TDS experiments could be performed under line of sight conditions. In this second chamber the sample could be cooled down with He to 40 K. High purity gases were used in the experiments: H<sub>2</sub> purity 5.3, NO purity 2.5 (both LINDE). All pressures given in this paper were corrected with the different ionization probabilities, of the gases, i.e.,  $S_{H_2}/S_{N_2} = 0.45$  and  $S_{NO}/S_{N_2} = 1.2$ . The Rh(110) sample which had a diameter of  $\approx 8$  mm was the same as used in previous experiments.<sup>8,11,13-15</sup> Prior to each experiment the sample was cleaned by a combination of Ar ion sputtering (1 kV) at 770 K, annealing to 1200 °C followed by an oxygen treatment at 1070 K ( $p_{O_2} = 1 \times 10^{-6}$  mbar,  $t=5$  min) and a second annealing to 1470 K.

## III. RESULTS

### A. Coadsorption and titration experiments

*In situ* LEED experiments conducted under reaction conditions between  $\approx 500$  and 600 K revealed that essentially three types of structures are involved in the formation of chemical wave patterns: O-induced reconstructions, N-induced reconstructions, and a mixed N,O overlayer. Typically a  $c(2 \times 6)$ -O, a  $(2 \times 1)/(3 \times 1)$ -N, and a mixed  $c(2 \times 4)$ -2O,N structure are observed.<sup>14</sup> Since the width of the pulses ( $\approx 10$ – $50 \mu\text{m}$ ) which appear as traveling white bands in PEEM is much smaller than the diameter of the LEED beam ( $\approx 0.5$ – $1$  mm), the LEED pattern displays a superposition of the various structures. Based on their different work function values we can nevertheless assign the dark area in PEEM to the  $c(2 \times 6)$ -O and  $c(2 \times 4)$ -2O,N and the bright stripes to the  $(2 \times 1)/(3 \times 1)$ -N with some possible contribution of the adsorbate free surface.

Apparently the excitation mechanism for pulses in the system Rh(110)/NO+H<sub>2</sub> consists of a sequence of structural transformations leading from the  $c(2 \times 6)$ -O via the  $(2 \times 1)/(3 \times 1)$ -N of adsorbed nitrogen back to the oxygen covered sur-

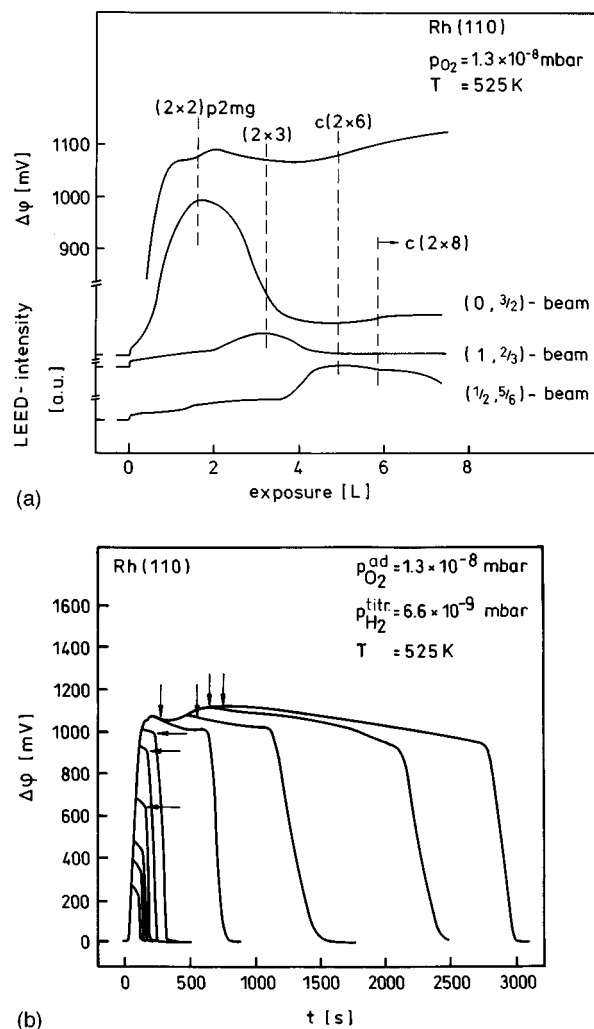


FIG. 1. Inhibition of the O<sub>2</sub>+H<sub>2</sub> reaction at high oxygen coverages. (a) Uptake curves for oxygen showing the variation of the work function ( $\Delta\phi$ ) and the development of ordered overlayers in LEED. The  $(0, \frac{3}{2})$ -beam belongs to the  $(2 \times 2)p2mg$  and to the  $c(2 \times 8)$  but the first relative maximum is entirely due to the  $(2 \times 2)p2mg$ . The  $(1, \frac{2}{3})$ -beam is part of the  $c(2 \times 6)$  and of the  $(2 \times 3)$ , since, however, the  $(\frac{1}{2}, \frac{5}{6})$ -beam belongs only to the  $c(2 \times 6)$  one can separate the two contributions. (b) Titration of the partially oxygen covered Rh(110) surface with hydrogen. After adsorption of O<sub>2</sub> the oxygen was turned off and H<sub>2</sub> was introduced. The arrows mark the beginning of the titration with H<sub>2</sub>.

face. The position and the role of the mixed  $c(2 \times 4)$ -2O,N remains to be specified. Dynamical LEED analyses have been conducted for the  $(2 \times 1)/(3 \times 1)$ -N, the  $c(2 \times 4)$ -2O,N, and for the  $(2 \times 2)p2mg$ -O which is similarly built as the  $c(2 \times 6)$ -O.<sup>6-9</sup> These results together with a number of STM investigations provide a detailed picture of all the relevant surface structures in the reaction system but what is less clear are the different adsorption properties of these structures and their stability in a reacting environment. In order to answer some of these questions a number of simple adsorption and titration experiments were conducted.

Figure 1(a) displays the  $\Delta\phi$ -uptake curve during oxygen adsorption at  $T=525$  K, and in addition to  $\Delta\phi$  the intensities of some selected LEED beams are reproduced which monitor the development of the ordered oxygen adlayers. Above

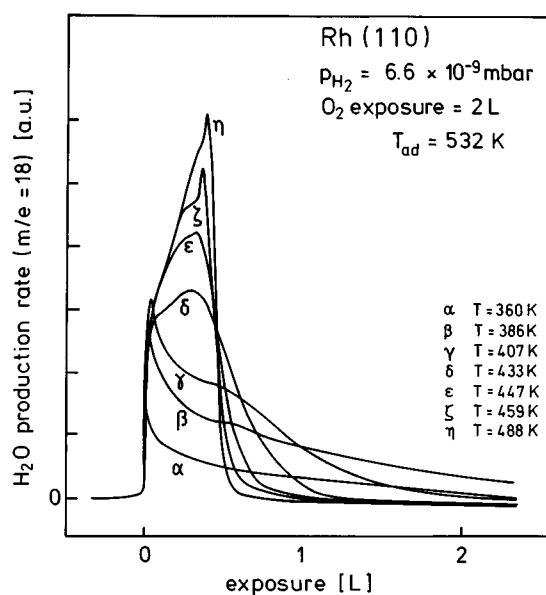


FIG. 2. Titration of an oxygen covered Rh(110) surface with hydrogen at various temperatures.

480 K adsorption of oxygen leads to various O-induced reconstructions which are all based on the missing row building principle and whose phase diagram has been studied in detail before.<sup>1,2,6,30</sup> One notes that the steep linear  $\Delta\phi$  increase takes place already before completion of the  $(2\times 2)p2mg$  corresponding to  $\theta_0=0.5$ . The further uptake of oxygen up to nearly a monolayer [ $c(2\times 8)\text{-O}$ ] causes only a small  $\Delta\phi$  variation. At very high oxygen exposures (not shown in the diagram) a  $np(10\times 16)$  pattern develops as reported before.<sup>30</sup>

As one now modifies the previous experiment by interrupting the flow of oxygen at certain points and exposing the partially oxygen covered surface to hydrogen, one obtains the titration curves displayed in Fig. 1(b). Similar to the uptake curves the titration curves exhibit two sharply distinct slopes. The almost plateaulike part of the  $\Delta\phi$  traces becomes increasingly long as the initial oxygen coverage is increased beyond that of the  $(2\times 2)p2mg$ . Clearly the long plateaulike parts of the  $\Delta\phi$  traces reflect a strong inhibition of hydrogen adsorption by oxygen which apparently starts at oxygen coverages beyond  $\theta_0\sim 0.5$ .

The reaction between oxygen and hydrogen exhibits a pronounced temperature dependence as demonstrated by the data in Fig. 2 showing the titration of a  $(2\times 2)p2mg$  oxygen adlayer at temperatures between 360 K and 488 K. At low temperatures between 360 K and 407 K the H<sub>2</sub>O reaction rate exhibits its highest value at the beginning of the titration and then drops off continuously. With increasing temperature a relative rate maximum develops at 0.3 L H<sub>2</sub> exposure (488 K), whose height grows with temperature. At the highest temperature, at  $T=488$  K, the rate increases steadily up to that maximum and then drops off sharply to a near zero level. The position of the relative maximum is shifted only slightly to higher H<sub>2</sub> exposures with increasing temperature. An evaluation of the desorption rate reveals that the reactive

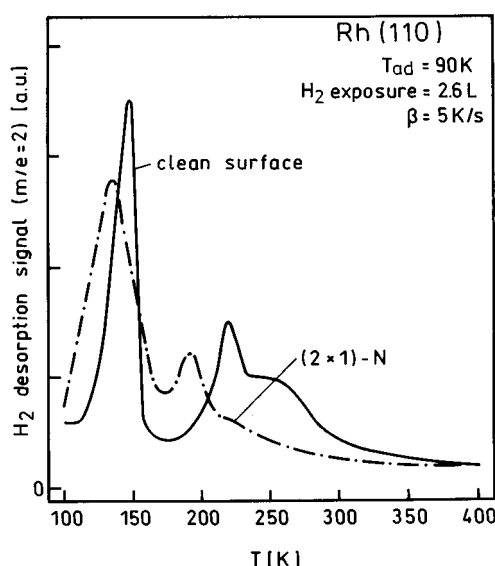


FIG. 3. Comparison of the H<sub>2</sub> TD spectra from a clean surface and a surface with a  $(2\times 1)\text{-N}$  overlayer of adsorbed nitrogen (Ref. 31).

sticking coefficient at the absolute rate maximum (curve  $\eta$ ) roughly equals one with an estimated uncertainty of  $\approx 30\%$ .

A simple explanation for the increase of the reaction rate with decreasing oxygen coverage (at  $T>407$  K) is the removal of the inhibitory effect of higher oxygen coverages on the adsorption of hydrogen [see Fig. 1(b)]. The fact that this increase in the reaction rate is only seen at  $T\geq 433$  K can be attributed to the experimental observation that oxygen and Rh atoms in the Rh(110)/O system only become mobile at  $T>430$  K.<sup>30</sup> Such a mobility is, however, required if an adlayer in a titration experiment is to reduce its coverage uniformly instead of allowing a "hole-eating" mechanism.

In the chemical wave patterns pulses are traveling across the surface which, due to their reduced work function, were assigned to an essentially nitrogen covered  $(2\times 1)/(3\times 1)\text{-N}$  surface with some possible contribution of the bare Rh(110) surface.<sup>14,15</sup> In order to determine the reactivity and stability of the nitrogen adlayer against the two reactants, H<sub>2</sub> and NO, a well-ordered  $p(2\times 1)\text{-N}$  structure was prepared. The procedure involved an exposure of the Rh(110) surface at  $T=520$  K to an NO/H<sub>2</sub> atmosphere with  $p_{\text{NO}}=1\times 10^{-8}$  mbar and  $p_{\text{H}_2}=1\times 10^{-6}$  mbar for 150 s followed by a cooling down to 90 K. At this temperature the sample was exposed to 2.6 L H<sub>2</sub> and the resulting TD spectrum is reproduced together with the H<sub>2</sub> TDS of the clean surface in Fig. 3.<sup>31</sup> Although the total amount of adsorbed hydrogen is only slightly affected by preadsorbed nitrogen, the adsorption states are modified very strongly. The more strongly bound TD states above 200 K are almost completely suppressed by nitrogen whereas the low temperature state is broadened and a new state at 190 K is formed. Since under reaction conditions at  $T>500$  K the surface residence time and hence the availability of adsorbed hydrogen is mainly determined by the high temperature adsorption states, the data shown in Fig. 3 suggest a certain reduction of the reactivity of small amounts of

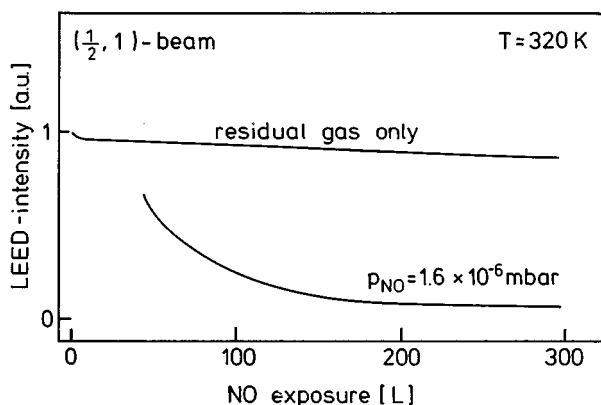


FIG. 4. LEED experiment showing the removal of the  $(2 \times 1)$ -N structure of nitrogen by adsorbing NO. The  $(\frac{1}{2}, 1)$ -beam intensity monitors the amount of the  $(2 \times 1)$ -N overlayer. The intensity decrease which results from residual gas adsorption during 5 min exposure time has been included in the diagram.

coadsorbed oxygen to H<sub>2</sub> in the  $(2 \times 1)$ -N as compared to the situation on a clean Rh(110) surface.

The adsorption of the second gas, NO, onto the  $(2 \times 1)$ -N at  $T=320$  K is shown in Fig. 4. In contrast to H<sub>2</sub> adsorption which does not affect the ordering in the N-adlayer, NO adsorption destroys the  $(2 \times 1)$ -N structure. At  $T=320$  K this happens, however, relatively slow since the data in Fig. 4 demonstrate that more than 55 L NO are required to decrease the intensity of a fractional order beam of the  $(2 \times 1)$ -N by 50%. At  $T=320$  K no new structure was discernible in LEED forming after destruction of the  $(2 \times 1)$ -N but a decrease in the integral order intensity indicated a disordered surface.<sup>32</sup> The destruction of the  $(2 \times 1)$ -N by adsorbing NO is consistent with the results of STM measurements of NO adsorption on Rh(110), demonstrating that the  $(2 \times 1)$ -N which initially is present is removed as the substrate with rising oxygen coverage is forced into a  $1 \times 2$  "missing row" reconstruction.<sup>4,5</sup>

The structure which is formed finally upon NO adsorption onto the clean surface at 300 K is a mixed  $c(2 \times 4)$ - $2O, N$  adlayer whose substrate exhibits the same,  $1 \times 2$  "missing row" reconstruction as in the  $(2 \times 2)p2mg$ -O structure of pure oxygen.<sup>4,5</sup> For this mixed overlayer structure a dynamical LEED analysis was conducted, showing that the two oxygen atoms per unit cell occupy the three fold fcc sites similar to the  $(2 \times 2)p2mg$  while the nitrogen atom is located at the bottom of the "1x2" valley bridging two Rh atoms.<sup>8</sup> Each adsorbate thus retains the same local adsorption geometry it has in the pure adsorbate structures, i.e., in the  $(2 \times 2)p2mg$ -O and in the  $(2 \times 1)$ -N.<sup>6-9</sup> It is therefore important to know how the coadsorption with nitrogen modifies the reactivity of the oxygen atoms.

To answer this question a  $c(2 \times 4)$ - $2O, N$  was prepared and heated up in a hydrogen atmosphere while monitoring the formation of the reaction products H<sub>2</sub>O ( $m/e=18$ ) and N<sub>2</sub> ( $m/e=28$ ). For comparison this experiment was repeated with a  $(2 \times 2)p2mg$ -O structure which exhibits the same substrate structure and contains the same number of oxygen at-

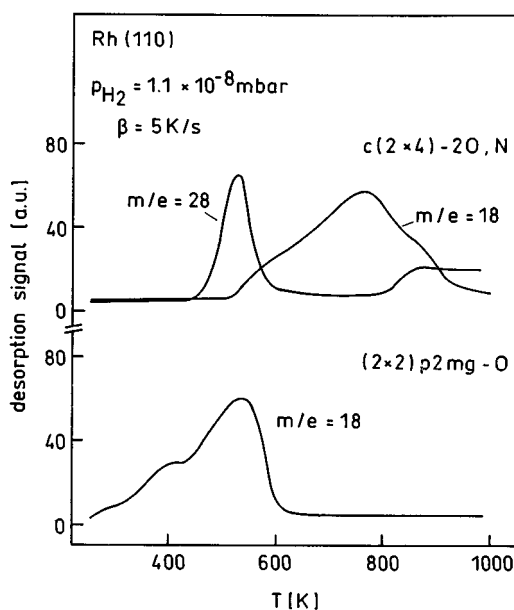


FIG. 5. Temperature programmed reaction (TPR) experiments showing the different reactivity of the  $(2 \times 2)p2mg$  of pure oxygen and of the  $c(2 \times 4)$ - $2O, N$  with a mixed overlayer. After adjusting a fixed  $p_{H_2} = 1.1 \times 10^{-8}$  mbar, both structures were heated up in a hydrogen atmosphere with a constant heating rate while monitoring the production of N<sub>2</sub> ( $m/e=28$ ) and H<sub>2</sub>O ( $m/e=18$ ).

oms. The TD spectra displayed in Fig. 5 demonstrate that H<sub>2</sub>O formation in the pure oxygen adlayer already sets in at 300 K whereas in the mixed adlayer H<sub>2</sub>O is formed only beyond 500 K. The comparison with the N<sub>2</sub> production rate shows that H<sub>2</sub>O only starts to form after most of the nitrogen is desorbed, thus indicating that it is the nitrogen in the mixed overlayer which inhibits the reaction of oxygen with hydrogen.

In a chemical wave the nitrogen coverage varies between zero and 0.5. The decisive factor controlling the stability of the nitrogen is, however, less the reactivity toward hydrogen which is rather low as evidenced by the previous experiment but the desorption of nitrogen. The varying stability of adsorbed nitrogen was demonstrated by Comelli *et al.* who showed that the nitrogen in the mixed  $c(2 \times 4)$ - $2O, N$  is strongly destabilized by coadsorbed oxygen leading to an N<sub>2</sub> TD-peak in between  $\approx 450$  and 600 K.<sup>24,26</sup> This  $T$ -range roughly coincides with the  $T$ -range for chemical wave patterns.<sup>14</sup> As shown by Fig. 6 the N<sub>2</sub> TD spectra from a  $(2 \times 1)$ -N structure exhibit a quite different behavior following a zeroth order desorption kinetics with the peak maximum shifted up to 620 K for the fully nitrogen covered surface. The enormous shift in the peak maximum from 525 K in the  $c(2 \times 4)$ - $2O, N$  to 620 K in the  $(2 \times 1)$ -N, which was noted in earlier investigations, is apparently essential for the stability of these structures under reaction conditions and thus a key element of the excitation/oscillation mechanism.

## B. Stationary reaction conditions

Figure 7 shows the work function variation as a Rh(110) is heated cyclewise in a NO/H<sub>2</sub> atmosphere with  $p_{H_2}/p_{NO}$

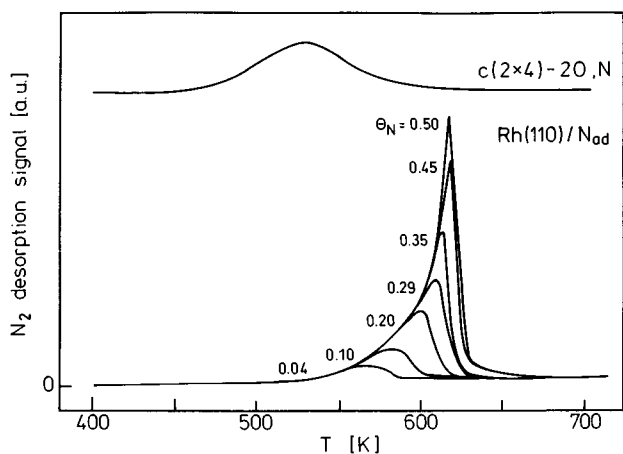


FIG. 6. Effect of coadsorbed oxygen on the stability of adsorbed nitrogen. The diagram shows a comparison of N<sub>2</sub> TD spectra of a mixed  $c(2 \times 4)$ -2O,N-overlayer (top) with desorption from a purely nitrogen covered surface (bottom). The nitrogen adlayers were prepared by exposing the surface at  $T=520$  K to a NO/H<sub>2</sub> mixture with a large excess of hydrogen (see text). In this way ordered  $(3 \times 1)/(2 \times 1)$ -N overlayers are formed with the fully developed  $(2 \times 1)$ -N corresponding to  $\theta_N=0.50$ .

= 14:1. The  $\Delta\phi$  trace displays three distinct work function levels which we can assign to the oxygen covered, the nitrogen covered, and the bare Rh(110) surface. These assignments are based on work function measurements of the individual adsorbate structures demonstrating that the high oxygen coverage phases, i.e., the  $c(2 \times 6)$ -O and the  $c(2 \times 8)$ -O and the mixed  $c(2 \times 4)$ -2O,N phase both exhibit work function values between 1000 and 1100 mV while the  $p(2 \times 1)$ -N displays a work function change of 280 mV. The existence range for chemical wave patterns lies in the transition region between the  $\Delta\phi$  levels of the N- and of the O-covered surface.

The connection between different adsorbate structures on Rh(110) and their catalytic activity is demonstrated in Fig. 8 where the LEED intensities and the N<sub>2</sub> production rate have been recorded simultaneously during a heating/cooling cycle in a NO/H<sub>2</sub> atmosphere. Shown are the intensities of

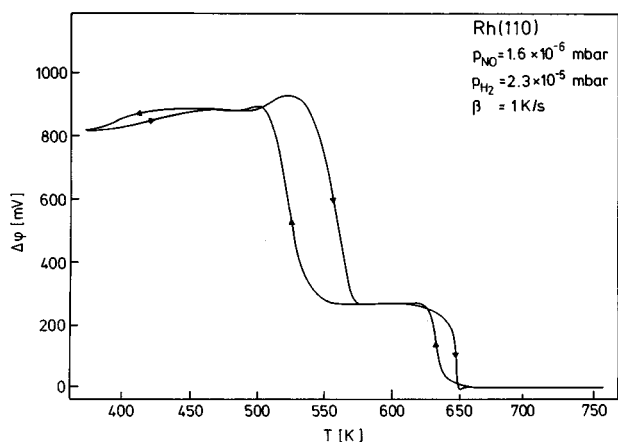


FIG. 7. Variation of the work function during a heating/cooling cycle in a NO/H<sub>2</sub> atmosphere.

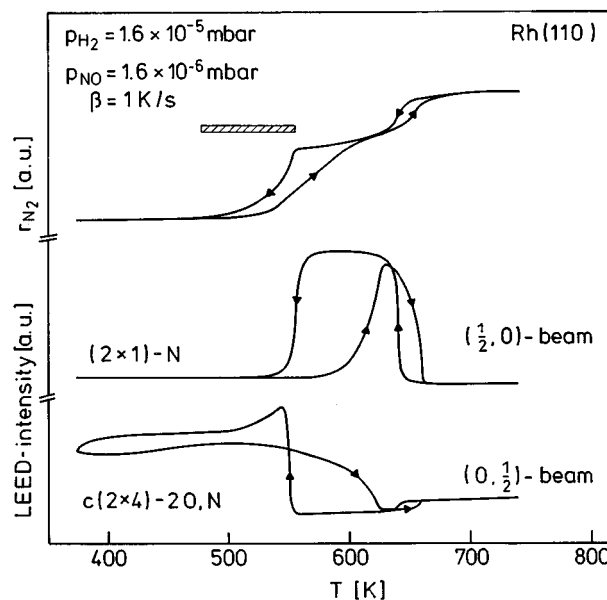


FIG. 8. Correlation between the catalytic activity and the changes in the surface structure during a heating/cooling cycle in a NO/H<sub>2</sub> atmosphere. Shown are the N<sub>2</sub> production rate,  $r_{N_2}$ , and the variation in the intensity of the  $(\frac{1}{2}, 0)$ -beam monitoring the  $(2 \times 1)$ -N structure and in the  $(0, \frac{1}{2})$ -beam intensity representing the mixed  $c(2 \times 4)$ -2O,N overlayer. The  $(0, \frac{1}{2})$  beam also contains intensity from the  $c(2 \times 8)$ -O, but this contribution is rather small. Indicated as shaded area in the diagram is also the existence range for pattern formation which was taken from Ref. 14.

the  $(1/2, 0)$  beam of the  $(2 \times 1)$ -N and of the  $(0, 1/2)$  beam which is part of the  $c(2 \times 4)$ -2O,N and of the  $c(2 \times 8)$ -O pattern. The contribution of this latter structure is, however, rather small. Similar to the  $\Delta\phi$  trace, the reaction rate exhibits three distinct plateaus and we can assign the highest reactivity to the bare surface, the intermediate reactivity to the  $(2 \times 1)$ -N of adsorbed nitrogen, and the lowest reactivity to the high oxygen coverage phases, i.e., to the mixed  $c(2 \times 4)$ -2O,N, the  $c(2 \times 8)$ -O, and to the  $c(2 \times 6)$ -O which was not monitored in that particular experiment.

These assignments agree qualitatively well with the observations made in the titration experiments. The high oxygen coverage phases and the  $c(2 \times 4)$ -2O,N were found to inhibit H<sub>2</sub> adsorption [see Figs. 1(b) and (5)] whereas the  $(2 \times 1)$ -N exhibited H<sub>2</sub> adsorption states which were merely shifted down to lower temperature (see Fig. 3). Neglecting a possible contribution from structural imperfections and adsorbate free surface area, the data in Fig. 8 indicate that the reactivity of the  $(2 \times 1)$ -N is almost  $\frac{2}{3}$  of that of the clean surface present above 650 K.

Variation of  $p_{H_2}$  has mainly an effect on the width of the  $T$ -window for the  $(2 \times 1)$ -N in a heating/cooling cycle experiment. So a decrease of  $p_{H_2}$  by a factor of  $\approx 3$  causes a strong shrinking of the existence range for the  $(2 \times 1)$ -N while a  $p_{H_2}$  increase has the opposite effect. The dependence of the reaction rate on  $p_{H_2}$  is displayed for three different temperatures,  $T=540$ , 580, and 620 K in Fig. 9. The rate curves exhibit essentially two activity levels: a low level state connected with an oxygen covered surface and a reactive state

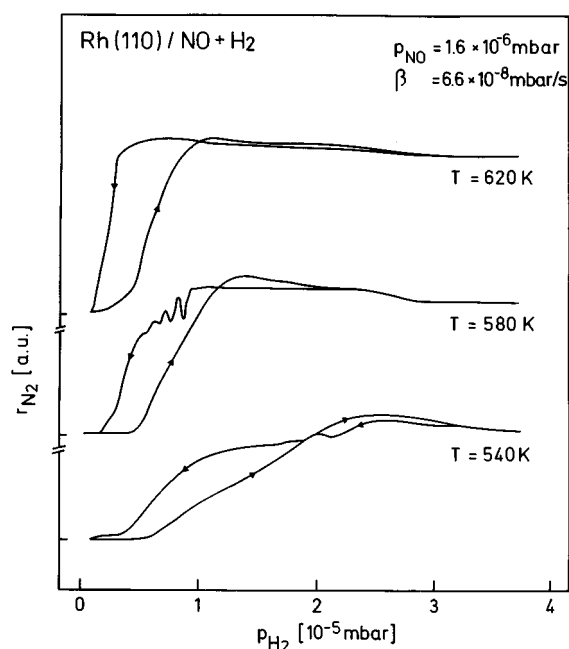
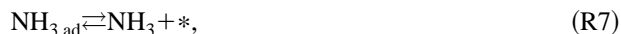
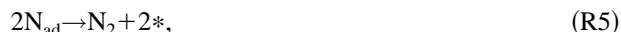
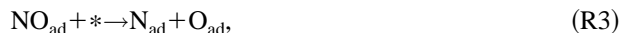


FIG. 9. Dependence of the N<sub>2</sub> production rate,  $r_{N_2}$ , on the hydrogen partial pressure at different temperatures. The curve was recorded by cycling  $p_{H_2}$  while the temperature and  $p_{NO}$  were kept constant.

associated with the nitrogen covered and/or bare surface, respectively. Lowering the temperature affects the two rate levels only slightly but the transition range widens and with it the existence range for chemical wave patterns.

#### IV. DISCUSSION

The following mechanistic scheme can be formulated for the NO+H<sub>2</sub> reaction on Rh(110):



(\* denotes a vacant adsorption site).

In this scheme intermediates in H<sub>2</sub>O and NH<sub>3</sub> formation have been neglected and different types of sites in the substrate structure were not taken into account. In our experimental

setup NH<sub>3</sub> and N<sub>2</sub>O formation were not detected but these products have been observed in experiments with other Rh surfaces, i.e., on Rh(111) and Rh(533).<sup>21-23</sup>

Molecularly adsorbed NO undergoes dissociation above 170 K but higher adsorbate coverages were found to have a strongly inhibiting effect on NO dissociation.<sup>33</sup> Above 400 K, however, no molecular NO species was detected on Rh(110) and we can therefore assume that under the reaction conditions considered here step (R3) is always fast.<sup>28,33</sup> The “surface explosion” mechanism, i.e., the rapid dissociation of NO caused by an autocatalytic increase in the number of vacant sites which was shown to be the essential driving force for oscillations in the NO+CO and NO+H<sub>2</sub> reaction on Pt(100) can therefore be put aside here.<sup>34</sup>

Atomic oxygen and nitrogen formed by dissociation of NO both penetrate into the subsurface region of Rh(110) producing subsurface oxygen (O<sub>sub</sub>) and subsurface nitrogen (N<sub>sub</sub>). On Rh(110) this was demonstrated directly with x-ray photoelectron spectroscopy (XPS) and also indirectly in work function studies.<sup>17,28</sup> However, no quantitative data are available that would allow one to derive the kinetics and the energetic parameters of the corresponding segregation equilibria and to estimate the contribution of adsorbate-adsorbate interactions forcing the adparticles into subsurface sites. In particular, no data exist showing how the adsorption properties and the reactivity of the Rh(110) surface are modified by the presence of subsurface oxygen/nitrogen. Such an information would, however, be essential for the construction of an oscillatory mechanism based on the reversible formation of a subsurface species analogous to the oscillation mechanism suggested for Pd(110)/CO+O<sub>2</sub>.<sup>35</sup>

Since the system Rh(110)/NO+H<sub>2</sub> involves a number of different reconstructions depending on the N- and O-coverage, the operation of reconstruction mechanism analogous to the oscillation mechanism for catalytic CO oxidation on Pt(100) and Pt(110) appears in principle to be feasible.<sup>34</sup> There the change in the oxygen sticking coefficient between the CO-stabilized 1×1 phase and the reconstructed surface was shown to be the essential driving force for the rate oscillations. In the system considered here the adsorption of hydrogen and nitrogen on a Rh(110)-(1×1) and a metastable (1×2) “missing row” reconstructed surface have been investigated, but the differences in the adsorption properties were not very pronounced so that the construction of an oscillation mechanism analogous to that for catalytic CO oxidation on Pt(100) and Pt(110) appears to be unrealistic.<sup>27</sup>

An indication of what could be the driving force for the oscillations in the Rh(110)/NO+H<sub>2</sub> system comes from a different set of experiments. Rate oscillations in the NO+H<sub>2</sub> reaction have also been found on Rh(111) and Rh(533).<sup>21,22</sup> PEEM measurements revealed that traveling pulses with similar width and velocity as on Rh(110) can be observed on these surfaces.<sup>23</sup> Similar to Rh(110) the existence ranges for oscillations and pattern formation lie in a temperature range where the TD peaks of nitrogen are found. No oscillations in the NO+H<sub>2</sub> reaction have been found on Rh(100), which differs from the other surfaces by a nitrogen adsorption state

which is particularly tightly bound and which desorbs by more than 100 K higher than nitrogen adsorbed on Rh(110) and Rh(111).<sup>21,22</sup>

These results already indicate that the stability of the nitrogen adlayer plays a key role in the oscillation mechanism. Further support for this hypothesis comes from some very detailed investigations by Kiskinova *et al.* and by Comelli *et al.* who studied the effect of coadsorbed oxygen on the stability of nitrogen adlayers.<sup>24–26</sup> They found that large quantities of coadsorbed oxygen have a strongly destabilizing effect on the N-adlayer whereas small amounts of oxygen stabilize the N-adlayer. This shows up clearly in N<sub>2</sub> TD spectra and the corresponding data are displayed in Fig. 6 showing spectra of the  $c(2\times 4)$ -2O,N and of the  $(2\times 1)$ -N. Nitrogen from a  $(2\times 1)$ -N desorbs with zeroth order kinetics and a TD maximum at 620 K while nitrogen from the mixed  $c(2\times 4)$ -2O,N structure desorbs with a peak maximum at 525 K. The high stability of nitrogen in the  $(2\times 1)$ -N can be attributed to the formation of the Rh-N-Rh chains which are absent in the  $c(2\times 4)$ -2O,N.<sup>3,8</sup> The zeroth order kinetics which the data from the  $(2\times 1)$ -N clearly demonstrate can be explained with the dissolution of the  $(2\times 1)$ -N islands starting from the ends of these chains.

In order to construct a complete oscillation cycle one has to explain what factors first stabilize and then destabilize the  $(2\times 1)/(3\times 1)$ -N structure on Rh(110). In experiments in which the N-adlayer was produced by dosing NH<sub>3</sub> on a Rh(110) surface precovered with oxygen Kiskinova *et al.* observed a strong upward shift of the N<sub>2</sub> TD peak compared to adsorption on a clean surface.<sup>26</sup> They explained this shift with a stabilizing effect of small amounts of oxygen on the N-adlayer and they assumed that the oxygen is preferentially located in subsurface sites.

One possible way to explain the stabilizing effect of small oxygen coverages is that the oxygen allows an improved ordering of the N-adlayer leading to the formation of large  $(2\times 1)/(3\times 1)$ -N islands.<sup>3</sup> On the other hand, there is little doubt that oxygen and nitrogen penetrate into the deeper layers of Rh(110) and that this will also affect the adsorption and catalytic properties of Rh(110). The influence of a subsurface species on the adsorption properties is, however, difficult to determine experimentally and since no experimental facts are known momentarily which either prove or rule out a decisive role of the subsurface species in the oscillation mechanism, we do not present here a detailed mechanistic model and leave out a possible influence of subsurface oxygen or subsurface nitrogen.

Titration experiments with hydrogen as shown in Figs. 1(b) and 5 and also the results of measurements under stationary reaction conditions displayed in Figs. 7–9 demonstrate that the structures with a high oxygen coverage, i.e., the  $c(2\times 6)$ -O and the mixed  $c(2\times 4)$ -2O,N exhibit a low catalytic activity whereas the  $(2\times 1)/(3\times 1)$ -N is fairly reactive. PEEM measurements of the O<sub>2</sub>+H<sub>2</sub> reaction on Rh(110) have shown bistability with reaction reaction fronts initiating transitions between an unreactive high coverage oxygen phase and a reactive low coverage oxygen phase.<sup>29</sup> Based on these results and on LEED observations published

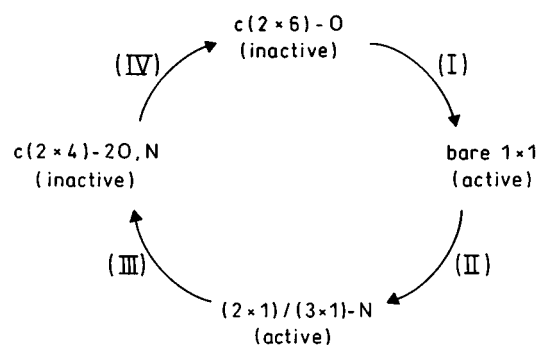


FIG. 10. Proposed sequence of structural transformations in a chemical wave in the system Rh(110)/NO+H<sub>2</sub>.

earlier showing that essentially three types of structures are seen in the pattern forming parameter range, i.e., a  $c(2\times 6)$ -O, a  $(2\times 1)/(3\times 1)$ -N and a mixed  $c(2\times 4)$ -2O,N, the following oscillation/excitation cycle can be constructed. This scheme depicted in Fig. 10 consists of four steps:

- (1) Starting with a fully oxygen covered surface H<sub>2</sub> adsorption and hence the reaction are inhibited. Creation of a few adsorption sites probably by reaction at some structural defects will initiate the rapid reactive removal of the oxygen. This happens in a reaction which is autocatalytic due to the self-accelerating increase in the number of vacant adsorption sites. An essentially adsorbate free surface is created which plays the role of a short-living intermediate. The coupling between the autocatalytic reaction and the surface diffusion of hydrogen will create a propagating reaction front.
- (2) On the bare Rh(110) surface NO can adsorb and dissociate uninhibitedly. Since oxygen is removed reactively as H<sub>2</sub>O by coadsorbing hydrogen this will lead to an enrichment of nitrogen and hence the formation of a  $(2\times 1)/(3\times 1)$ -N structure.
- (3) If we assume that the reactivity of the  $(2\times 1)/(3\times 1)$ -N is sufficiently reduced not to remove all of the oxygen which is formed by dissociating NO then the accumulation of oxygen will destroy the pure nitrogen structure and cause the formation of a mixed  $c(2\times 4)$ -2O,N structure.
- (4) Nitrogen coadsorbed with oxygen is not bound strongly and therefore N<sub>2</sub> desorption will initiate a transformation of the mixed  $c(2\times 4)$ -2O,N structure into a pure oxygen structure, i.e., into the  $c(2\times 6)$ -O. Thus the oscillation cycle is completed.

The scheme depicted in Fig. 10 contains two elements which lack a direct experimental proof. The existence of a bare Rh(110) surface did not show up directly in the experimental LEED data, but on the other hand the rapid reactive removal of the oxygen adlayer has to create such an intermediate. Furthermore, no direct experimental proof exists that the mixed  $c(2\times 4)$ -2O,N develops under pattern forming conditions after disappearance of the  $(2\times 1)/(3\times 1)$ -N and not before or parallel to this structure. Under oscillatory condi-



tions, however, LEED showed that the (2×1)-N spots appear before the *c*(2×4)-2O,N structure develops. Both structures are then simultaneously present. Furthermore, since large amounts of coadsorbed oxygen destabilize adsorbed nitrogen there is little choice in constructing a meaningful cycle besides the scheme given in Fig. 10.

The transformation of a (2×1)/(3×1)-N structure with rising oxygen coverage into a mixed *c*(2×4)-2O,N structure has been demonstrated also in STM measurements of NO adsorption on Rh(110).<sup>4,5</sup> While at low NO exposure atomic oxygen and nitrogen formed separate (2×1)/(3×1)-N and 1×2 reconstructed oxygen islands, high coverages forced the adsorbates into a common *c*(2×4)-2O,N overlayer with a (1×2) "missing row" reconstructed substrate geometry. In the experiments performed here the destruction of a (2×1)-N adlayer by adsorbing NO was demonstrated by the LEED data depicted in Fig. 4.

In the scheme given above the principle mechanism is the change of the stability of a nitrogen adlayer caused by coadsorbed oxygen. One could suspect that the same change between an oxygen and a nitrogen covered surface also holds for the system Rh(111)/NO+H<sub>2</sub> but different from Rh(110) on this surface only a (2×2) pattern originating from adsorbed oxygen has been observed so far.<sup>23</sup> So far no adsorbate-induced reconstructions are known for Rh(111)/N,O. This could be taken as evidence that details of the surface structure are probably of minor importance for the oscillation mechanism but that it is rather the general stabilizing or destabilizing interaction between coadsorbed oxygen and nitrogen which appears to be decisive. The presence of subsurface oxygen or subsurface nitrogen could play a key role in this interaction but this is an open question which remains to be solved in future experiments.

## V. CONCLUSIONS

The stability and reactivity of the adsorbate structures which are present in the pattern forming parameter range of the NO+H<sub>2</sub> reaction on Rh(110) has been investigated. It was shown that the phases with a high oxygen coverage, i.e., the *c*(2×6)-O and the mixed *c*(2×4)-2O,N exhibit a strongly reduced reactivity due to the inhibition of hydrogen adsorption. Quite in contrast, the catalytic activity of the (2×1)/(3×1)-N of nitrogen is only slightly reduced compared to the clean surface. NO adsorption causes the destruction of the (2×1)/(3×1)-N phase. The binding strength of adsorbed nitrogen is strongly affected by coadsorbed oxygen. An excitation mechanism for chemical waves is suggested consisting of the sequence *c*(2×6)-O, bare 1×1, (2×1)/(3×1)-N, *c*(2×4)-2O,N, *c*(2×6)-O. Essential for this mechanism is the stabilization and destabilization, respectively of adsorbed nitrogen by coadsorbed oxygen. The role of subsurface oxygen and subsurface nitrogen remains to be shown.

## ACKNOWLEDGMENT

The authors are indebted to S. Wasle for preparation of the drawings.

- <sup>1</sup>F. M. Leibsle, P. W. Murray, S. M. Francis, G. Thornton, and M. Bowker, *Nature* **363**, 706 (1993).
- <sup>2</sup>P. M. Murray, F. M. Leibsle, Y. Li, Q. Guo, M. Bowker, G. Thornton, V. R. Dhanak, K. C. Prince, and R. Rosei, *Phys. Rev. B* **47**, 12976 (1993).
- <sup>3</sup>P. W. Murray, F. M. Leibsle, G. Thornton, M. Bowker, V. R. Dhanak, A. Baraldi, M. Kiskinova, and R. Rosei, *Surf. Sci.* **304**, 48 (1994).
- <sup>4</sup>P. W. Murray, G. Thornton, M. Bowker, V. R. Dhanak, A. Baraldi, R. Rosei, and M. Kiskinova, *Phys. Rev. Lett.* **71**, 4369 (1993).
- <sup>5</sup>V. R. Dhanak, A. Baraldi, R. Rosei, M. Kiskinova, P. W. Murray, G. Thornton, and M. Bowker, *Phys. Rev. B* **50**, 8807 (1994).
- <sup>6</sup>A. Comicioli, V. R. Dhanak, G. Comelli, C. Astaldi, K. C. Prince, R. Rosei, A. Atrei, and E. Zanazzi, *Chem. Phys. Lett.* **214**, 438 (1993).
- <sup>7</sup>M. Gierer, H. Over, G. Ertl, H. Wohlgenuth, E. Schwarz, and K. Christmann, *Surf. Sci.* **297**, L73 (1993).
- <sup>8</sup>M. Gierer, F. Mertens, H. Over, G. Ertl, and R. Imbihl, *Surf. Sci.* **339**, L903 (1995).
- <sup>9</sup>V. R. Dhanak, A. Baraldi, G. Comelli, K. C. Prince, and R. Rosei, *Phys. Rev. B* **51**, 1965 (1995).
- <sup>10</sup>F. Mertens and R. Imbihl, *Nature* **370**, 124 (1994).
- <sup>11</sup>N. Gottschalk, F. Mertens, M. Bär, M. Eiswirth, and R. Imbihl, *Phys. Rev. Lett.* **73**, 3483 (1994).
- <sup>12</sup>A. S. Mikhailov, *Phys. Rev. E* **49**, 5875 (1994).
- <sup>13</sup>F. Mertens, N. Gottschalk, M. Bär, M. Eiswirth, A. Mikhailov and, R. Imbihl, *Phys. Rev. E* **51**, R5196 (1995).
- <sup>14</sup>F. Mertens and R. Imbihl, *Surf. Sci.* **347**, 355 (1995).
- <sup>15</sup>F. Mertens and R. Imbihl, *J. Chem. Phys.* **105**, 4317 (1996).
- <sup>16</sup>V. Schmatloch and M. Kruse, *Surf. Sci.* **296/270**, 488 (1992).
- <sup>17</sup>V. Schmatloch, I. Jirka, S. Heinze, and N. Kruse, *Surf. Sci.* **331-333**, 23 (1995).
- <sup>18</sup>S. Heinze, V. Schmatloch, and N. Kruse, *Surf. Sci.* **341**, 124 (1995).
- <sup>19</sup>M. F. H. van Tol, A. Gielbert, and B. E. Nieuwenhuys, *Appl. Surf. Sci.* **67**, 179 (1993); *Catal. Lett.* **16**, 297 (1992).
- <sup>20</sup>A. R. Cholach, M. F. H. van Tol, and B. E. Nieuwenhuys, *Surf. Sci.* **320**, 281 (1994).
- <sup>21</sup>N. M. H. Janssen, B. E. Nieuwenhuys, M. I. Kai, K. Tanaka, and A. R. Cholach, *Surf. Sci.* **319**, L29 (1994).
- <sup>22</sup>N. M. H. Janssen, P. D. Lobden, B. E. Nieuwenhuys, M. Ikai, M. Mukai, and K. Tanaka, *Catal. Lett.* **35**, 155 (1995).
- <sup>23</sup>N. M. H. Janssen, A. Schaak, B. E. Nieuwenhuys, and R. Imbihl, *Surf. Sci.* **364**, L555 (1996).
- <sup>24</sup>G. Comelli, S. Lizzit, Ph. Hofmann, G. Paolucci, M. Kiskinova, and R. Rosei, *Surf. Sci.* **277**, 31 (1992).
- <sup>25</sup>S. Lizzit, G. Comelli, Ph. Hofmann, G. Paolucci, M. Kiskinova, and R. Rosei, *Surf. Sci.* **276**, 144 (1992).
- <sup>26</sup>M. Kiskinova, S. Lizzit, G. Comelli, G. Paolucci, and R. Rosei, *Appl. Surf. Sci.* **64**, 185 (1993).
- <sup>27</sup>A. Baraldi, V. R. Dhanak, G. Comelli, K. C. Prince, and R. Rosei, *Surf. Sci.* **293**, 246 (1993).
- <sup>28</sup>A. Baraldi, V. R. Dhanak, M. Kiskinova, and R. Rosei, *Appl. Surf. Sci.* **78**, 445 (1994).
- <sup>29</sup>F. Mertens and R. Imbihl, *Chem. Phys. Lett.* **242**, 221 (1995).
- <sup>30</sup>H. Wohlgenuth, Thesis, FU Berlin, 1994.
- <sup>31</sup>M. Ehsasi and K. Christmann, *Surf. Sci.* **194**, 172 (1988).
- <sup>32</sup>R. J. Baird, R. C. Ku, and P. Wynblatt, *Surf. Sci.* **97**, 346 (1980).
- <sup>33</sup>V. Schmatloch, I. Jirka, and N. Kruse, *J. Chem. Phys.* **100**, 8471 (1994).
- <sup>34</sup>R. Imbihl and G. Ertl, *Chem. Rev.* **95**, 697 (1995).
- <sup>35</sup>S. Ladas, R. Imbihl, and G. Ertl, *Surf. Sci.* **219**, 88 (1989).